Photomechanical Properties of Rhodium(I)–Semiquinone Complexes. The Structure, Spectroscopy, and Magnetism of (3,6-Di-*tert*-butyl-1,2-semiquinonato)dicarbonylrhodium(I)

Christopher W. Lange,[1a] Maria Földeàki,[1b] V. I. Nevodchikov,[1c] V. K. Cherkasov,[1c] G. A. Abakumov,*[,1c] and Cortlandt G. Pierpont*[,1a]

Contribution from the Department of Chemistry and Biochemistry, University of Colorado, Boulder, Colorado 80209, Institute of Organometallic Chemistry, Academy of Sciences of the USSR, Nizhni Novgorod, USSR, and Materials Reliability Division, National Institute of Standards and Technology, Boulder, Colorado 80303. *Received August 28, 1991*

Abstract: Crystals of $Rh(CO)_2$(3,6-DBSQ) [3,6-DBSQ = 3,6-di-*tert*-butyl-1,2-semiquinone] have been reported to bend reversibly when exposed to light in the near-IR. Structural characterization on the complex has confirmed the Rh^I–DBSQ charge distribution for the complex and shown that molecules are stacked in columns in the solid state with a slightly nonlinear oligomeric rhodium core. Magnetic features show marked temperature dependence with both ferromagnetic and antiferromagnetic interactions apparent over the temperature range between 330 and 5 K. Coupling between radical semiquinone ligands is propagated through Rh–Rh interactions along the column. Solution (pentane) UV–vis-NIR spectra recorded over the temperature range from 300 to 150 K show evidence for oligomer formation with spectral changes resulting in a dramatic color change for the solution, from orange-brown at room temperature to dark green at lower temperatures. Strong transitions that appear in the NIR in solution at the lower temperatures also appear in the solid-state spectrum of the complex at room temperature. These properties reflect the strength of interactions between $Rh(CO)_2$(3,6-DBSQ) molecules in the polymeric chain. The low-energy MLCT transition that is characteristic of the oligomeric structure may contribute to the unique photomechanical property of the complex in the solid state.

Introduction

Many of the interesting and important features of transition metal complexes containing catecholate and semiquinone ligands are related to the similarity in energy between the quinone π^*-orbitals and the metal d-levels. This property is responsible for intense, low-energy charge-transfer transitions that sometimes extend well into the near-infrared (NIR).[2] Several years ago crystals of a semiquinone complex of a platinum group metal were reported to bend reversibly when exposed isothermally to low energy light.[3] Maximum sensitivity was found for light in the NIR with wavelengths in the 1200–1400-nm range, and the bending effect could be induced thermally. The complex that was the subject of this report is $Rh(CO)_2$(3,6-di-*tert*-butyl-1,2-semiquinone).[4] Experiments have been carried out on $Rh(CO)_2$(3,6-DBSQ) in both the solid state and in solution to study properties that might contribute to this unusual behavior.

Experimental Section

Samples of $Rh(CO)_2$(3,6-DBSQ) were prepared using procedures described previously.[4] Long thin crystals were formed by cooling a saturated pentane solution of the complex.

Physical Measurements. Magnetic measurements were made using a Quantum Design SQUID Magnetometer. Variable temperature UV–vis-NIR spectra were recorded on a Perkin Elmer Lambda 9 spectrophotometer equipped with a RMC-Cryosystems cryostat. Standard 1.0-cm solution cells were used.

Crystallographic Structure Determination on $Rh(CO)_2$(3,6-DBSQ). Crystals of $Rh(CO)_2$(3,6-DBSQ) form as long thin needles that are dark red-brown in color. Few of the single crystals formed had sufficient volume for crystallographic investigation. One of the larger crystals obtained by recrystallization from pentane solution was mounted and aligned on a Siemens P3/F diffractometer. Photographs obtained on the crystal indicated triclinic symmetry, and a full sphere of data was collected using θ–2θ scans within the angular range between 3° and 50° in 2θ. A summary of crystallographic data is given in Table I. The structure was solved using a combination of direct and Patterson methods. Two independent complex molecules were located, stacked along the crystallographic *a*-axis. The locations of the four Rh atoms within the unit cell is pseudomonoclinic. However, the monoclinic symmetry is broken by the locations of the ligand atoms. Final cycles of full-matrix least-squares refinement converged with discrepancy indices of $R = 0.060$ and $R_w = 0.076$. Atomic coordinates, tables containing detailed procedures used in the structure determination, full listings of bond distances and angles, atomic anisotropic displacement parameters, and hydrogen atom locations are available as supplementary material. Selected bond lengths and angles are given in Table II.

Table I. Crystallographic Data for $Rh(CO)_2$(3,6-DBSQ)[a]

mol wt	379.2
color	brown
crystal system	triclinic
space group	$P\bar{1}$
a (Å)	6.551 (3)
b (Å)	11.640 (5)
c (Å)	23.063 (9)
α (deg)	75.60 (3)
β (deg)	83.34 (4)
γ (deg)	78.64 (4)
vol. (Å^3)	1665.9 (12)
Z	4
D_{calcd} (g cm^{-3})	1.512
μ (mm^{-1})	1.019
T_{min}, T_{max}	0.714, 0.988
R, R_w	0.060, 0.076
GOF	0.95

[a] Radiation, Mo Kα (0.71073 Å); temperature, 294–297 K.

Table II. Average Bond Distances and Angles for $Rh(CO)_2$(3,6-DBSQ)

	Lengths (Å)		
Rh–O	2.026 (4)	C1–C2	1.453 (15)
Rh–C	1.844 (9)	C2–C3	1.426 (10)
C–O_{CO}	1.139 (11)	C3–C4	1.352 (10)
C1–O_{SQ}	1.295 (8)	C4–C5	1.414 (15)
	Angles (deg)		
O–Rh–O	79.9 (3)	O–Rh–C	95.5 (5)
C–Rh–C	89.2 (6)	O–Rh–C	175.5 (5)
Rh–C–O_{CO}	177.3 (9)		

Experimental Results

Crystals of $Rh(CO)_2$(3,6-DBSQ) form as long, thin triclinic needles in space group $P\bar{1}$ with two independent molecules of the

(1) (a) University of Colorado, Boulder. (b) NIST, Boulder. (c) Institute of Organometallic Chemistry, Nizhni Novgorod.
(2) Haga, M.; Dodsworth, E. S.; Lever, A. B. P.; Boone, S. R.; Pierpont, C. G. *J. Am. Chem. Soc.* **1986**, *108*, 7413.
(3) Abakumov, G. A.; Nevodchikov, V. I. *Dokl. Akad. Nauk SSSR* **1982**, *266*, 1407.
(4) Nevodchikov, V. I.; Abakumov, G. A.; Cherkasov, V. K.; Razuvaev, G. A. *J. Organomet. Chem.* **1981**, *214*, 119.

0002-7863/92/1514-4220$03.00/0

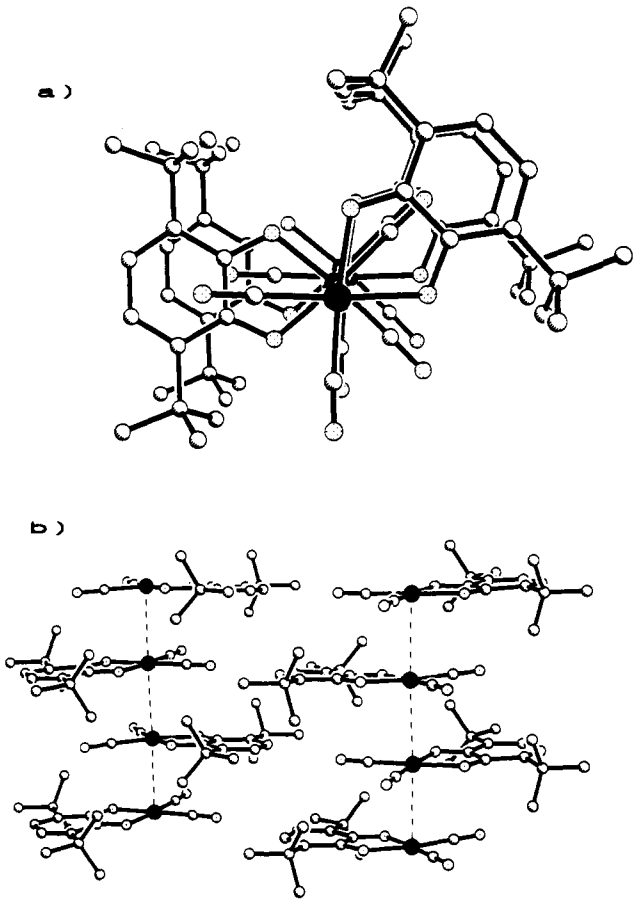

Figure 1. (a) View of $Rh(CO)_2(3,6\text{-DBSQ})$ down the crystallographic a^* axis. (b) View showing the alignment of molecular columns within the unit cell.

complex per unit cell. Planar complex molecules form in columns with metal atoms located atop one another as shown in Figure 1. Within the unit cell pairs of centrosymmetrically related molecules define parallel columns. Rhodium atoms that form the core of a column are not perfectly aligned atop one another with angles between Rh–Rh vectors and complex planes that range from 86.6° to 88.8°. Separations between Rh atoms are 3.252 (4) and 3.304 (5) Å, values that agree with Rh–Rh separations found for other stacked Rh(I) dimers and oligomers.[5] Metrical dimensions for the quinone ligands are typical of coordinated semiquinones with an average C–O length of 1.295 (8) Å and C–C lengths within the ring that show slight contraction at the C3–C4 and C5–C6 bond positions of the 3,6-DBSQ ligand. The average Rh–O length to the semiquinone oxygen atoms is 2.026 (4) Å, and the Rh–C lengths to the carbonyl ligands average to 1.844 (9) Å.

Magnetic measurements on $Rh(CO)_2(3,6\text{-DBSQ})$ show evidence for both ferromagnetic and antiferromagnetic interactions. Magnetic susceptibility plotted as a function of temperature, recorded at a magnetic field strength of 10 kG, is shown in Figure 2. A similar result was obtained at a field of 20 kG including the discontinuity below 100 K. The temperature dependence of susceptibility from 330 K to approximately 104 K may be fit to a Curie–Weiss plot with a θ value of +20.7 K indicating the presence of a ferromagnetic interaction. Magnetic moment remains relatively constant over this temperature range, increasing slightly from 0.99 to 1.09 μ_B per Rh, values that reflect a competing antiferromagnetic interaction. A decrease in magnetization

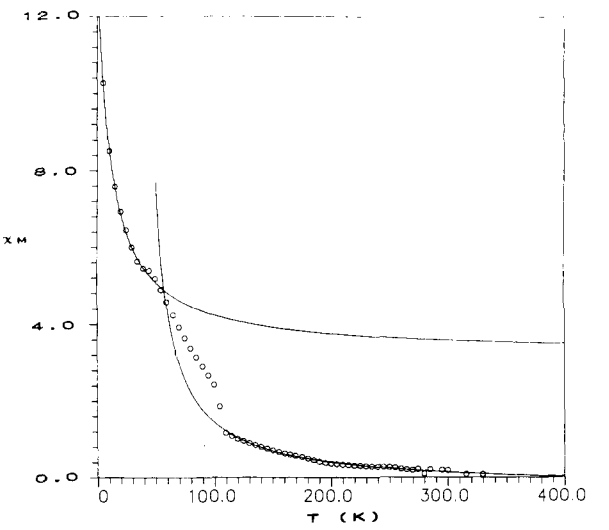

Figure 2. Plot of magnetic susceptibility ($m^3\ mol^{-1}$, $\times 10^5$) of $Rh(CO)_2(3,6\text{-DBSQ})$ versus temperature. Solid lines represent theoretical plots for ferromagnetic ($T > 100$ K) and antiferromagnetic ($T < 50$ K) coupling based on Curie–Weiss behavior.

with decreasing field strength measured at 200 K confirms the predominant ferromagnetic character of the interaction at higher temperatures. At 105 K there is a sharp increase in magnetic susceptibility and magnetic moment that appears to result from ferromagnetic ordering. Magnetic moment increases to 1.49 μ_B before the increase in susceptibility is quenched at lower temperatures by antiferromagnetic coupling. Low temperature data shown in Figure 2 may be fit to a Curie–Weiss plot with a value for θ of −11.7 K, with a drop in magnetic moment to 0.63 μ_B at 5.0 K.

Radical semiquinone ligands are the paramagnetic centers of the individual complex units in the molecular chains. The complicated magnetic behavior in solid state indicates the presence of, at least, three types of intermolecular interactions within and, possibly, between chains of molecules. Direct interaction between radical ligands separated by more than 7 Å along the column would be weak, and the magnetic behavior of $Rh(CO)_2(3,6\text{-DBSQ})$ demonstrates the strength of intermolecular communication through the metal core of the molecular column. In toluene solution at room temperature $Rh(CO)_2(3,6\text{-DBSQ})$ shows a three line EPR spectrum due to coupling with the two equivalent hydrogen atoms at the four- and five-ring positions of the semiquinone ligand.[6] As temperature is lowered the spectrum disappears. UV–vis-NIR spectra of the complex show reversible dependence upon concentration and temperature. Spectra recorded in pentane solution at room temperature show a MLCT band at 430 nm that has been assigned as the $2a_1(d_{z^2}) \rightarrow 2b_1(\pi^*(SQ))$ transition.[7] As the temperature of the solution is decreased new bands appear in the visible and NIR regions with the development of a broad, intense transition at 1500 nm as the lowest energy transition. This band increases in intensity to 150 K, our low-temperature limit. Spectra recorded on solid samples of $Rh(CO)_2(3,6\text{-DBSQ})$ also show a broad transition centered at 1550 nm as the lowest energy transition with higher energy bands at 295, 470, and 790 nm. The temperature and concentration dependence of the solution spectra result from concatenation of complex molecules to give stacked oligomers. As stacks form, interacting d_{z^2} orbitals combine to form filled band levels of higher and lower energy. Simple Hückel theory may be used to model spectral shifts associated with the oligomerization process.[8] With the assumption that the transition at 430 nm cor-

(5) (a) Zakarov, L. N.; Struchkov, Yu. T.; Abakumov, G. A.; Nevodchikov, V. I. *Koord. Khim.* **1990**, *16*, 1101. (b) Gordon, G. C.; DeHaven, P. W.; Weiss, M. C.; Goedken, V. L. *J. Am. Chem. Soc.* **1978**, *100*, 1003. (c) Takenaka, A.; Sasada, Y.; Omura, T.; Ogoshi, H.; Yoshida, Z.-I. *J. Chem. Soc., Chem. Commun.* **1973**, 792. (d) Bailey, N. A.; Coates, E.; Robertson, G. B.; Bonati, F.; Ugo, R. *J. Chem. Soc., Chem. Commun.* **1967**, 1041.

(6) Abakumov, G. A.; Nevodchikov, V. I.; Cherkasov, V. K. *Izvest. Akad. Nauk SSSR, Ser. Khim.* **1988**, 1411.

(7) Abakumov, G. A.; Nevodchikov, V. I.; Cherkasov, V. K. *Izvest. Akad. Nauk SSSR, Ser. Khim.* **1985**, 2709.

(8) (a) Mann, K. R.; Gordon II, J. G.; Gray, H. B. *J. Am. Chem. Soc.* **1975**, *97*, 3553. (b) Lewis, N. S.; Mann, K. R.; Gordon II, J. G.; Gray, H. B. *J. Am. Chem. Soc.* **1976**, *98*, 7461.

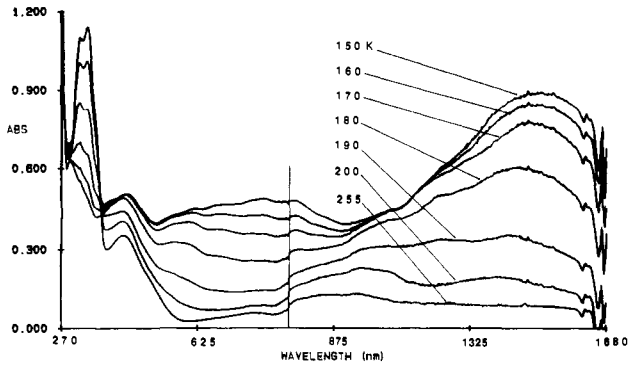

Figure 3. Electronic spectrum of $Rh(CO)_2(3,6\text{-DBSQ})$ recorded in pentane solution (1.58×10^{-4} M) over the temperature range from 255 to 150 K.

responds to the $d_{z^2} \rightarrow \pi^*(SQ)$ transition of the $Rh(CO)_2(3,6\text{-DBSQ})$ monomer ($E°$) and that the transition at 1500 nm is the related transition for the $[Rh(CO)_2(3,6\text{-DBSQ})]_n$ limiting oligomer ($E° + 2\beta$), the value for the resonance integral associated with energy of the interaction between d_{z^2} orbitals may be estimated. This value, 18 700 cm^{-1}, may, in turn, be used to calculate the positions of bands associated with the dimer, trimer, tetramer, and higher order oligomers. Calculated values of 965 (dimer), 1186 (trimer), and 1296 nm (tetramer) all have corresponding transitions that appear through the temperature range as shown in Figure 3. However, they do not account for all spectral changes that occur as temperature is decreased. A dramatic decrease in intensity of sharp, intense transitions at 320 and 340 nm is observed with an increase in absorption in the region between 500 and 900 nm due to the appearance of four or five new transitions of lower intensity. These changes are responsible for a dramatic change in the color of the solution as temperature is decreased, from orange-red to dark green.

Conclusions

Temperature-dependent changes in electronic spectrum in solution result from catenation of complex units in stacked oligomers that are likely similar in structure to the form of the complex seen in the solid state. Magnetic behavior in the solid state is complicated, but it shows the effects of strong magnetic interactions between paramagnetic radical ligands within the stacks of staggered complex molecules. This interaction is propagated through the relatively weak Rh–Rh interactions that exist along the core of the molecular columns. An additional effect of the solid-state interactions is an unusually intense, low-energy electronic transition that does not appear for individual complex molecules.

The structural, spectral, and magnetic properties of $Rh(CO)_2(3,6\text{-DBSQ})$ are of interest, but it is unclear how they are related to the crystal bending effect. A model for the bending interaction may be envisioned, where transfer of charge from the high-energy Rh band-level to the quinone ligand strengthens and contracts the Rh stack on the irradiated side of the crystal. This view is probably too simple and fails to include the effects of solid-state discontinuities and defect structure that may contribute to the photomechanical properties in a significant way. Nevertheless, the interesting spectral, structural, and magnetic properties of the compound provide a starting point for understanding the unique photophysical behavior of $Rh(CO)_2(3,6\text{-DBSQ})$.

Acknowledgment. Support for the research carried out at the University of Colorado was provided by the National Science Foundation through Grants CHE 88-09923 and CHE 90-23636.

Registry No. $Rh(CO)_2(3,6\text{-DBSQ})$, 69650-57-3.

Supplementary Material Available: Tables giving crystal data and details of the structure determination, atomic coordinates, anisotropic thermal parameters, hydrogen atom locations, bond lengths and angles for $Rh(CO)_2(3,6\text{-DBSQ})$ (12 pages); table of observed and calculated structure factors (11 pages). Ordering information is given on any current masthead page.